Structure and dielectric/piezoelectric properties of LiNbO$_3$-doped BiScO$_3$–PbTiO$_3$ ceramics with morphotropic phase boundary composition

Qiang Zhang · Zhenrong Li · Na Zhang · Zhuo Xu

Abstract 0.02LiNbO$_3$–0.98{(1 − x)BiScO$_3$–xPbTiO$_3$} (2LN–BS–xPT) ceramics near the morphotropic phase boundary (MPB) were investigated. MPB region of 2LN–BS–xPT ceramics was identified to be in the composition of 0.62 < x ≤ 0.64. The coexistence of the tetragonal domain structure and a polar microdomain structure was observed by transmission electron microscope for x = 0.64. It is found that 2LN–BS–xPT ceramics (x = 0.64) showed good piezoelectric and ferroelectric properties with piezoelectric constant d_{33} about 505 pC/N, planar electromechanical coupling factors k_p about 0.47, and remnant polarization P_r about 40 μC/cm^2, respectively, while T_{max} is about ∼350–400 °C. The high-temperature relaxation behavior was also studied in 2LN–BS–xPT ceramics. Effects of thermal depoling on the piezoelectric properties of 2LN–BS–xPT ceramics indicated good thermal stability before 300 °C for x = 0.62 and 0.64.

Introduction

Pb-based relaxor ferroelectrics have been of much attention due to their excellent properties. However, these Pb-based relaxor systems have relatively low Curie temperatures (T_c), for example lower than 200 °C for PMN–PT systems [1, 2] near the morphotropic phase boundary (MPB), which imposed great limitations on the temperature-dependent properties and polarization stability.

Q. Zhang · Z. Li (✉) · N. Zhang · Z. Xu
Electronic Materials Research Laboratory, Key Laboratory of the Ministry of Education and International Center for Dielectric Research, Xi'an Jiaotong University, Xi'an 710049, China
e-mail: zhrli@mail.xjtu.edu.cn

Recently, some high-temperature piezoelectric ceramics with high-temperature relaxation character based on BiScO$_3$–PbTiO$_3$ system have been developed, such as BiScO$_3$–PbTiO$_3$–(Ba, Sr)TiO$_3$ ternary system[3], BiScO$_3$–PbTiO$_3$–PbO·SnO$_2$ ternary system[4], and (Bi, Li)(Sc, Sb)O$_3$–PbTiO$_3$ ternary system[5], which are likely to be utilized in high-temperature piezoelectric application. Among them, (Bi, Li)(Sc, Sb)O$_3$–PbTiO$_3$ ceramics near MPB composition and 0.36BiScO$_3$–0.64{(1 − x)PbTiO$_3$–xLiNbO$_3$}(x = 0.04) ceramics [6] show relaxor ferroelectric features. The former was with T_{max} in the range of 300–340 °C, and piezoelectric and ferroelectric properties of d_{33} = 545 pC/N, k_p = 0.58, and P_r = 28.3 μC/cm^2. The latter was with T_{max} in the range of 300–340 °C [6] and d_{33} = 465 pC/N, k_p = 0.57, and P_r = 48 μC/cm^2, respectively. The high T_{max} of Bi-based perovskite structure relaxor ceramics is benefit for the higher temperature applications as comparison with PMN-PT relaxor ferroelectrics ceramics.

In this study, the relaxation behavior of 0.02LiNbO$_3$–0.98{(1 − x)BiScO$_3$–xPbTiO$_3$} (2LN–BS–xPT) ceramics had been identified. The phase structure and di-/piezoelectric properties of 2LN–BS–xPT ceramics were examined, which is similar to 0.36BiScO$_3$–0.64{(1 − x) PbTiO$_3$–xLiNbO$_3$} ceramics in Ref. [6]. But, in our study, the coexistence of the tetragonal domain structure and a polar microdomain structure was observed which are proved two-phase coexistence near MPB composition. Meanwhile, the relaxation properties of 2LN–BS–xPT (x = 0.62 and 0.64) ceramics would be also analyzed. Moreover, since the transducers and actuators usually needed to be operated over a broad temperature range [7], it is important to study the temperature-dependent properties for high-temperature relaxor ferroelectrics. Thus, the temperature dependence of piezoelectric response was

measured, which would be valuable for the applications of the high-temperature relaxor ferroelectrics in transducer and actuator.

Experimental procedure

Materials

Bi_2O_3 (99.0%), Li_2CO_3 (98.0%), Nb_2O_5 (99.0%), Sc_2O_3 (99.9%), TiO_2 (99.5%), and PbO (99.9%) powders were used as starting raw materials for 2LN–BS–xPT synthesis. All the raw materials were of analytical reagent (AR) grade.

Sample preparation

2LN–BS–xPT ($x = 0.58–0.66$) ceramics were prepared using the conventional mixed oxide method. The mixtures were ball-milled for 5 h in alcohol following by an oven drying, and the powders were calcined at 850 °C for 2 h in an aluminum crucible. And then the calcined powders were pressed into disks of 10 mm in diameter and about 1 mm in thickness, with polyvinyl alcohol (PVA) as binder. The pellets were sintered at 1050–1100 °C for 2 h in a sealed aluminum crucible to avoid the loss of PbO, Bi_2O_3, and Li_2CO_3 caused by sublimation.

Characterization

Phase structure of the sample was characterized using X-ray diffraction (XRD) (Rigaku D/MAX-2400, Rigaku). XRD patterns were calibrated with the internal standard, and peaks were obtained using Jade software (Materials Data Inc., Livermore, CA). Lattice parameters were calculated from the peaks using a least square minimization of errors. The microstructure of the fracture surface of 2LN–BS–PT ceramics was observed by scanning electron microscopy (SEM) (JSM-6360LV, JEOL). TEM studies were performed on some of the sintered samples with a transmission electron microscope (TEM, JEM-3010, bright-field imaging at an operating voltage of 300 kV, JEOL). It was mechanically polished down to about 30 μm, and then ion milled (Fischione 1010, USA) to make the samples electron transparent.

The d_{33} value was measured using a piezo-d_{33} meter (ZJ-3A) and the resonance frequency f_r and antiresonance frequency f_a were measured using a HP4294 analyzer. Dielectric measurements were performed with a HP4284A LCR meter from room temperature to 600 °C. High field polarization and strain behavior were determined using a modified Sawyer–Tower circuit and linear variable differential transducer driven by a lock-in amplifier (Stanford research system, model SR830). The thermal depoling experiments were conducted by holding the poled samples for 10 h at various high temperatures, cooling to room temperature, measuring their d_{33} and k_p value after 24 h.

Results and discussion

Phase structure and microstructure

Figure 1 shows the XRD patterns of sintered 2LN–BS–xPT ($x = 0.58–0.66$) ceramics. It is observed that the stable perovskite phases were obtained for all samples. For $x \leq 0.60$, the absence of (001) and (002) reflection peaks splitting shows a rhombohedral phase. For $x \geq 0.66$, the splitting of (001), (011), and (002) peaks indicates a tetragonal phase. From $x = 0.62$ to 0.64, (200) peaks undergo a change from gradually split to clearly split, demonstrating a phase transition from rhombohedral to tetragonal phases, which indicated that the MPB region located in $0.62 < x \leq 0.64$.

Figure 2 shows SEM photo of the fracture surface of $x = 0.64$ sample sintered at 1100 °C. It was found that there are no preferred grain growth orientation and little porosity. Figure 3 shows the TEM photo of the domain structure of unpoled sample for $x = 0.64$. It can be seen that the tetragonal domain structures are composed in $2^{\#}$ region. The domain width is ~0.06–0.2 μm, consistent with a grain size of ~4.0 μm [8] for $x = 0.64$ as shown in Fig. 2. Meanwhile, the rhombohedral domain structures consist of dark and white regions (in $1^{\#}$ region) as shown in Fig. 3, typical of a polar microdomain structure [9]. Hence, the ceramics near the MPB show the coexistence of the tetragonal domain structures and a polar microdomain structure for $x = 0.64$, which is similar to the coexistence
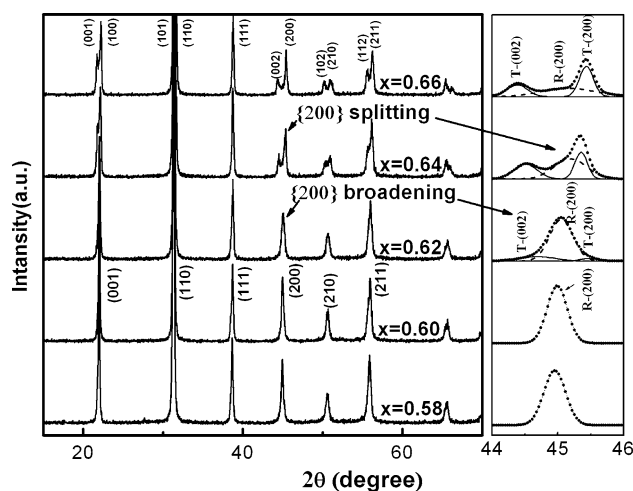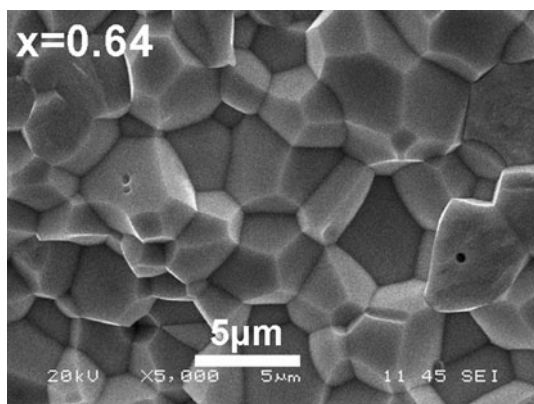

Fig. 1 XRD patterns of 2LN–BS–xPT ceramics

Fig. 2 SEM photo of 2LN–BS–0.64PT sample sintered at 1100 °C
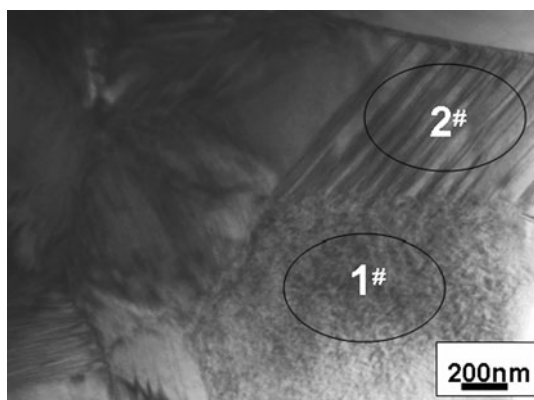

Fig. 3 TEM photos of 2LN–BS–0.64PT sample sintered at 1100 °C

of the tetragonal domain structures and a polar microdomain structure for BMT–0.38PT sample near the MPB [9].

Piezoelectric properties

The room-temperature piezoelectric constant (d_{33}) and the planar electromechanical coupling factors (k_p) for 2LN–BS–xPT ceramics with different PT content are showed in Fig. 4. The piezoelectric coefficient d_{33} is found to reach a maximum about 505 pC/N for $x = 0.64$, which is higher than for BS–0.64PT ceramics [10, 11], and k_p is about 0.47, indicating good piezoelectric properties near MPB region.

Dielectric properties

The temperature dependence of dielectric properties for 2LN–BS–xPT ($x = 0.60–0.66$) ceramics are shown in Fig. 5a–d. For $x = 0.66$, it indicated a diffuse phase transition. For $x = 0.60–0.64$, the maximum permittivity peaks decreased and the phase transition temperatures increased with the PT content increasing, while it exhibited high-temperature properties of T_{max} ∼350–400 °C and ε_{rmax}
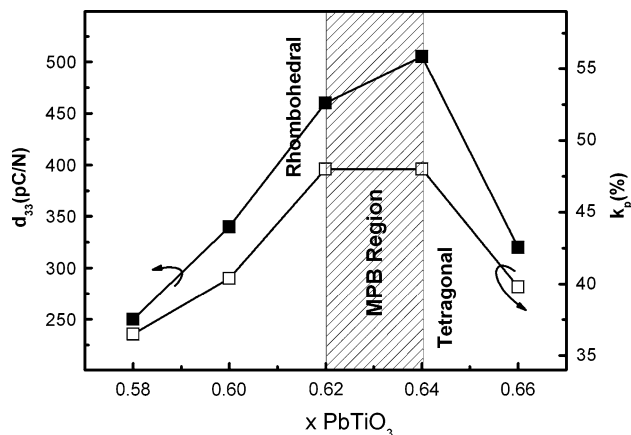

Fig. 4 Piezoelectric coefficient d_{33} and planar electromechanical couple factor k_p for 2LN–BS–xPT ceramics at room temperature

∼20000–22000. In Fig. 5, it can be seen that the temperature maxima of dielectric permittivity, T_{max}, shift to higher temperatures with increasing frequency, showing characteristic of a relaxor behavior. The emergence of the relaxor behavior caused by the addition of LN in the BS–PT ceramics is in accord with Setter et al.'s [12] and Bokov et al.'s [13] assumptions. According to their assumptions, the large differences in the valence between B′ and B″ ions and small size of A-site cation would enhance the elastic drive toward ordering on the B-site in A(B′B″)O$_3$ system, and the diffuse transition would be sharpened by increase in the B-cation ordering. In our study, it can be seen that the substitution of Li$^+$ on the A-site and Nb^{5+} on the B-site would apparently cause larger differences in the valence. Therefore, it can lead to a local disorder and the disruption of long-range order, which is likely to be a possible explanation for the relaxation for 2LN–BS–xPT system. For a ferroelectric material, Curie–Weiss law $1/\varepsilon = (T - T_o)/C'$ is obeyed for normal ferroelectric materials, including relaxor ferroelectrics, but only over the Burns temperatures T_{cw} [14, 15]. The terms in the equation are Curie–Weiss temperature of T_o (°C) and C' (°C), which is the Curie–Weiss constant. Figure 6a, b shows the plot of $1/\varepsilon$ versus T of 2LN–BS–xPT ($x = 0.62$ and 0.64) ceramics at 100 kHz. It is observed that it obeys the Curie–Weiss law above the Burns temperature (T_{cw}): 580 °C for $x = 0.62$, 570 °C for $x = 0.64$, respectively, and deviates from a linear fit below T_{cw}. Meanwhile, for $x = 0.62$ and 0.64, the parameters [($T - T_o$) vs. $1/\varepsilon$] obtained from the linear fit are $C' = 4.67 \times 10^5$ and 5.68×10^5, and $T_o = 448$ °C, respectively, which was consistent with a displacive phase transition from a high-temperature paraelectric phase to a ferroelectric phase.

The relaxation properties of 2LN–BS–xPT ($x = 0.62$ and 0.64) ceramics would be also analyzed by a modified Curie law, which can be written as [16, 17]:

Fig. 5 a–d Dielectric permittivity and dielectric loss as a function of temperature and frequency for 2LN–BS–xPT ceramics
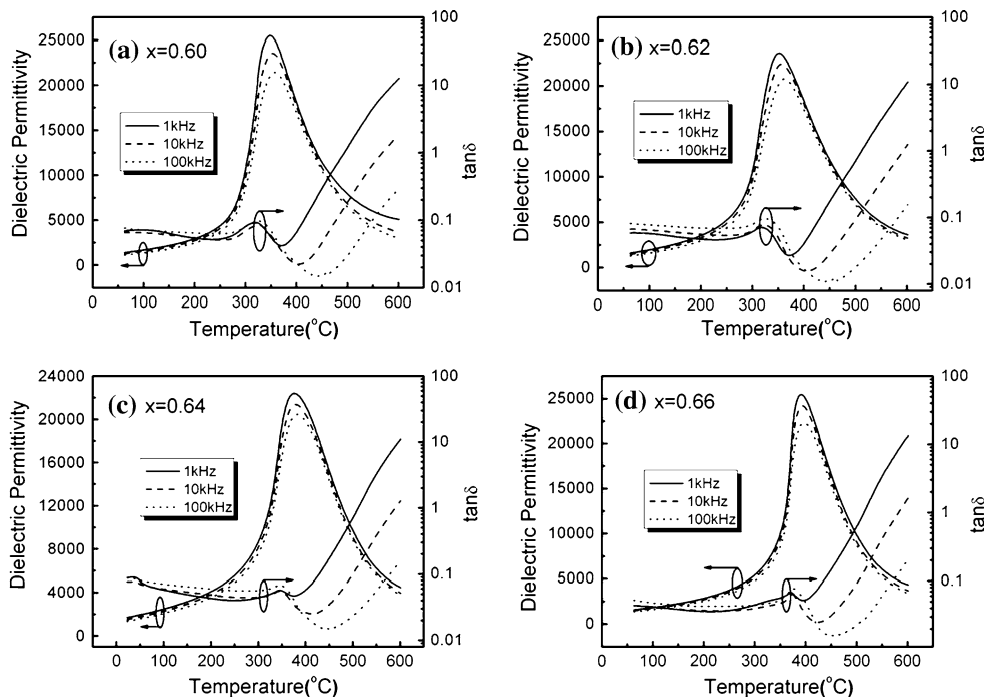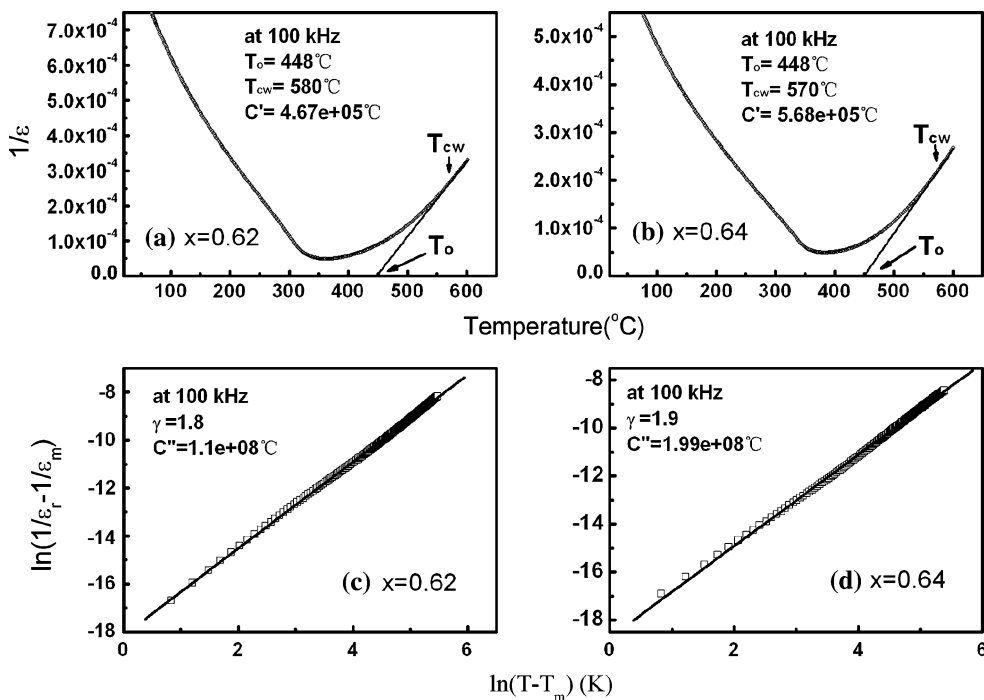

Fig. 6 Plots of **a** and **b** 1/ε versus T; **c** and **d** plots of ln (1/ε − 1/ε$_m$) versus ln(T − T$_m$) of 2LN–BS–xPT ceramics at 100 kHz

$$\frac{1}{\varepsilon} - \frac{1}{\varepsilon_m} = \frac{(T - T_m)^\gamma}{C''}, \tag{1}$$

where ε_m is the maximum value of the dielectric permittivity at the transition temperature T_m, C'' is the Curie-like constant which represents degree of diffuseness for transition peaks, and γ is the degree of diffuseness, where the value of γ varies between 1 and 2. Both γ and C'' were

determined from the slope and intercept of $\ln(1/\varepsilon - 1/\varepsilon_m)$ versus $\ln(T - T_m)$. The plots of $\ln(1/\varepsilon - 1/\varepsilon_m)$ versus $\ln(T - T_m)$ for 2LN–BS–xPT ceramics at 100 kHz are shown in Fig. 6c, d. By fitting the experimental data in Eq. 1, the values obtained for $\gamma = 1.8$ and 1.9, respectively, which indicated the diffuse phase transition for 2LN–BS–PT system.

Ferroelectric properties

At room temperature, bipolar polarization and strain hysteresis were measured at 30 kV/cm field and 0.5 Hz for 2LN–BS–xPT ceramics, as presented in Fig. 7a, b. According to Fig. 7, with the PT content increasing, coercive field (E_c) increased. For $x = 0.62$, the remnant polarization (P_r) reached a maximum of around 47 μC/cm^2, while coercive field (E_c) and strain are 19 kV/cm and 0.15%, respectively. Compared with BS–(0.62–0.66)PT ceramics ($P_r \sim 23$–32 μC/cm^2) [11], when a little substitution of LiNbO$_3$ ($x = 0.02$) doped into BS–PT, it can comparatively improve piezoelectric activity, indicating a general softening behavior.

The detailed dielectric and piezoelectric properties of 2LN–BS–xPT ceramics are summarized in Table 1. The properties showed a strong compositional dependence with the PT content and reached the maximum values close to MPB for $x = 0.62$ and 0.64. Combining with Figs. 1 and 3, the result of excellent piezoelectric properties near MPB is due to the existence of two thermodynamically equivalent phases which leads to the production of a highly domain-oriented material during the required poling process [18, 19]. In addition, we can easily conclude that 2LN–BS–xPT ceramics have better piezoelectric properties than PZT [20] and BS–0.64PT

[10], which would be valuable for the high-temperature applications of ferroelectric material. However, the dielectric loss of 2LN–BS–xPT ceramics is slightly large at room temperature.

Temperature dependence of piezoelectric properties

Figure 8a, b shows the effect of thermal depoling on the piezoelectric properties of 2LN–BS–xPT ceramics, expressed as relative changes from the room temperature values as defined:

$$\Delta d_{33}(T) = \frac{d_{33}(T) - d_{33}(RT)}{d_{33}(RT)} \times 100\%, \tag{2}$$

$$\Delta k_p(T) = \frac{k_p(T) - k_p(RT)}{k_p(RT)} \times 100\%, \tag{3}$$

where $d_{33}(RT)$ and $k_p(RT)$ are the value at room temperature, and $d_{33}(T)$ and $k_p(T)$ are measured at room temperature after 24 h when the poled samples were annealed for 10 h at the x-axis temperature. In Fig. 8a, b, for $x \leq 0.64$, the d_{33} values slightly decreased with the temperature up to ~ 300 °C, and then sharply dropped. For $x = 0.66$, d_{33} and k_p keep almost constant until 400 °C. 2LN–BS–xPT ceramics have excellent thermal stability and largely improved the usage temperature.

Fig. 7 Ferroelectric switching **a** polarization and **b** strain loops under bipolar drive for 2LN–BS–xPT ceramics at room temperature
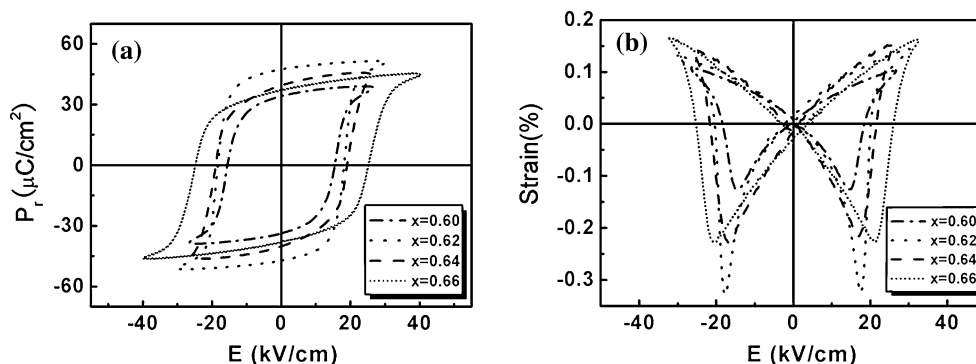

Table 1 Detailed piezoelectric and dielectric properties of 2LN–BS–xPT ceramics

Composition	Phase structure	T_{max} (°C)	K_{33}^T	Tanδ (at RT)	d_{33} (pC/N)	k_p	E_c (kV/cm)	P_r (μC/cm^2)	Strain (%)	Reference
Undoped PZT	MPB	~ 380	~ 730	–	223	0.53	–	0.20	–	[20]
BS-0.64PT	MPB	~ 450	~ 2010	0.02	460	0.56	20	32	0.25	[10]
BS–0.64PT–MnO$_2$	MPB	~ 445	~ 1540	0.01	390	0.56	22	30	–	[21]
BS–0.64PT–Nb$_2$O$_5$	MPB	~ 420	~ 1600	0.04	460	0.53	24	37	–	[22]
2LN–BS–xPT										
$x = 0.62$	Rhombohedral	~ 362	~ 1200	0.07	460	0.48	18	47	0.15	
$x = 0.64$	MPB	~ 383	~ 1570	0.07	505	0.47	19	40	0.15	
$x = 0.66$	Tetragonal	~ 397	~ 1300	0.03	360	0.40	27	39	0.15	

Fig. 8 Effect of thermal depoling on piezoelectric properties: **a** piezoelectric constant d_{33}; **b** planar electromechanical coupling factor k_p
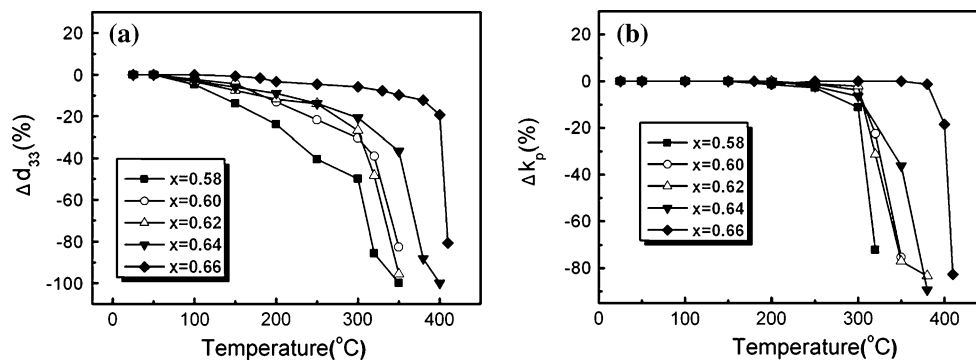
Conclusions

$0.02LiNbO_3$–$0.98\{(1 - x)BiScO_3$–$xPbTiO_3\}$ ceramics were studied. MPB region of 2LN–BS–xPT ceramics was identified to be in the composition of $0.62 < x \leq 0.64$. The coexistence of the tetragonal domain structures and a polar microdomain structure were observed in 2LN–BS–xPT ($x = 0.64$) ceramics. For $x = 0.64$, it showed good piezoelectric and ferroelectric properties ($d_{33} = 505$ pC/N, $k_p = 0.47$, and $P_r = 40$ μC/cm^2). High-temperature relaxor behavior was observed in 2LN–BS–xPT ceramics ($x = 0.60$–0.64), and it exhibited high-temperature properties of $T_{max} \sim 350$–400 °C for $0.60 \leq x \leq 0.64$. The piezoelectric properties of 2LN–BS–xPT ceramics decreased slightly below 300 °C for $x = 0.62$ and 0.64, while for $x = 0.66$, d_{33} and k_p keep almost constant until 400 °C. The results of thermal depoling experiments indicated that 2LN–BS–xPT ceramics have excellent thermal stability and largely improved the usage temperature, which would provide a proper solution for high-temperature transducer applications.

References

1. Choi SW, Shrout TR, Jang SJ, Bhalla AS (1989) Ferroelectrics 100:29
2. Wongmaneerung R, Yimnirun R, Ananta S (2009) J Mater Sci 44:5428. doi:10.1007/s10853-009-3621-6
3. Song TH, Eitel RE, Shrout TR, Randall CA, Hackenberger W (2003) Jpn J Appl Phys Part 1 42:5181
4. Song TH, Eitel RE, Shrout TR, Randall CA (2004) Jpn J Appl Phys 43:5392
5. Jiang Y, Zhao Y, Qin B, Jiang Y, Shi W, Li L, Xiao D, Zhu J (2008) Appl Phys Lett 93:022904
6. Chen Y, Zhu J, Xiao D, Qin B, Jiang Y (2009) J Alloy Compd 470:420
7. Shrout TR, Eitel R, Randall CA (2002) EPFL Swiss Federal Institute of Technology, Chap 19
8. Randall CA, Barber DJ, Whatmore RW (1987) J Mater Sci 22:925. doi:10.1007/BF01103531
9. Randall CA, Eitel R, Jones B, Shrout TR (2004) J Appl Phys 95:3633
10. Eitel RE, Randall CA, Shrout TR, Park SE (2002) Jpn J Appl Phys Part 1 41:2099
11. Eitel RE, Ransall CA, Shrout TR, Rehrig PW, Hackenberger W, Park SE (2001) Jpn J Appl Phys 40:5999
12. Setter N, Cross LE (1980) J Mater Sci 15:2478. doi:10.1007/BF00550750
13. Bokov AA, Ye Z-G (2006) J Mater Sci 41:31. doi:10.1007/s10853-005-5915-7
14. Burns G, Dacol FH (1983) Phys Rev B 28:2527
15. Viehland D, Jang SJ, Cross LE, Wuttig M (1992) Phys Rev B 46:8003
16. Rolovo BN (1965) Sov Phys Solid State 6:1676
17. Uchino K, Nomura S (1982) Ferroelectr Lett Sect 44:55
18. Isupov VA (1968) Sov Phys Solid State (Engl Transl) 10:989
19. Haertling GH (1999) J Am Ceram Soc 82:797
20. Jaffe B, Cook WR, Jaffe H (1971) Piezoelectric ceramics. Academic Press, Reported by R.A.N. Publishers, Marietta
21. Zhang SJ, Eitel RE, Randal CA, Shrout TR, Alberta EF (2005) Appl Phys Lett 86:262904
22. Chen S, Dong X, Yang WH, Liang R, Mao C (2007) J Am Ceram Soc 90:477